Modified DDV method of aerosol optical depth inversion over land surfaces from CBERS02B

WANG Zhong-ting[1,2], CHEN Liang-fu[2], GONG Hui[2,3,4], GAO Hai-liang[2,3,4]

1. *Satellite Environment Center, Ministry of Environmental Protection, Beijing* 100029, *China*;
2. *China State Key Laboratory of Remote Sensing Science, Jointly Sponsored by the Institute of Remote Sensing Applications of Chinese Academy of Sciences and Beijing Normal University, Beijing* 100101, *China*;
3. *Demonstration Center for Spaceborne Remote Sensing, National Space Administration, Beijing* 100101, *China*;
4. *Graduate University of Chinese Academy of Sciences, Beijing* 100039, *China*

Abstract: In this paper, the retrieval of AOD (aerosol optical depth) over land surfaces from CCD (Charge Coupled Device) data of CBERS (China Brazil Earth Resources Satellite) 02B was studied. The inversive method is modified DDV (dark dense vegetation) algorithm: (1) based on the spectral data of vegetation and the characteristics of the CCD sensor, the relationship between blue and red band surface reflectances and the NDVI (Normalized Difference Vegetation Index) thresholds for dense vegetation (dark pixel) were worked out, and the atmospheric effect and its correction were also analyzed. (2) The LUT (look up table) for different bands was pre-computed using the 6S atmospheric radiative transfer code. (3) The AODs was retrieved through interpolating in LUT in accordance with radiances obtained by CCD, and the errors of this modified DDV method was also analyzed and discussed. Finally, the modified DDV method was successfully applied to Nanning and Beijing areas. The comparison of the retrieved AODs with those of MODIS shows a good agreement.

Key words: remote sensing, CBERS02B, aerosol optical depth over land surfaces, dark dense vegetation

CLC number: P407/TP701 **Document code:** A

1 INTRODUCTION

It is difficult to retrieve aerosol over land surfaces from satellite data, because of the variety of aerosol physical and chemical properties, uneven distribution in spatio-temporal scale and the influence of land surfaces. Now, there are many methods for the aerosol properties retrieval, such as DDV (Kaufman & Sendra, 1988), contrast reduction (Tanré *et al*., 1988), the method based on global surface reflectance database (Hsu *et al*., 2004) and directional polarized method (Herman *et al*., 1997). In China, researches have been carried out on the MODIS aerosol product validation (Mao *et al*., 2002), the retrieval of surface reflectance and AOD simultaneously from space measurement over land (Duan *et al*., 2002), and aerosol optical depth retrieval from MODIS (Wang *et al*., 2003; Li *et al*., 2003). Nowadays, the China Brazil Earth Resources Satellite-CBERS02B data has been widely used in agriculture, land cover classification and forestry utilizations, etc. But few tests have been reported about the AOD inversion from this high spatial resolution data. In this paper, based on the calibration of the CCD data, the probability of retrieving AOD from CBERS02B CCD data was discussed over the experiment areas.

2 METHODOLOGY

2.1 Modified DDV method

The upward reflectance (normalized solar radiance), at the top of the atmosphere (TOA), is a function of successive orders of radiation interactions, within the coupled surface-atmosphere system (Vermote *et al*., 1997):

$$L(\mu_v) = L_0(\mu_v) + \frac{r}{1-rS}\mu_s F_0 T(\mu_s) T(\mu_v) \quad (1)$$

where, $\mu_s = \cos\theta_s$, $\mu_v = \cos\theta_v$, θ_s is solar zenith, θ_v is view zenith, $L_0(\mu_v)$ is atmospheric path reflectance, S is atmospheric backscattering ratio, T is atmospheric transmission, r is land reflectance and F_0 is TOA solar radiance.

Eq.(1) is normalized by $F_0\mu_s$ into Eq.(2):

$$\rho_{TOA}(\mu_s,\mu_v,\phi) = \rho_0(\mu_s,\mu_v,\phi) + \frac{T(\mu_s)T(\mu_v)\rho_s(\mu_s,\mu_v,\phi)}{[1-\rho_s(\mu_s,\mu_v,\phi)S]} \quad (2)$$

where, ϕ is relative azimuth angle and ρ_S is angular spectral surface reflectance.

Eq. (2) can be written in another form as:

Received: 2008-02-27; **Accepted**: 2008-09-01

Foundation: 863 project (No. 2006AA06A303) and Chinese Academy of Sciences major projects of knowledge innovation program (No: kzcx1-yw-06-01).

First author biography: WANG Zhong-ting (1980—), male, engineer, received the Ph. D. degree in Cartography and Geographical Information Systems in 2008 from Graduate School of Chinese Academy of Sciences. His researches focus on atmospheric aerrosol remote sensing inversion. He has published more than 10 papers.

$$\rho_{\mathrm{s}}(\mu_{\mathrm{s}},\mu_{\mathrm{v}},\phi)=\frac{\rho_{\mathrm{TOA}}(\mu_{\mathrm{s}},\mu_{\mathrm{v}},\phi)-\rho_0(\mu_{\mathrm{s}},\mu_{\mathrm{v}},\phi)}{T(\mu_{\mathrm{s}})T(\mu_{\mathrm{v}})+\rho_{\mathrm{TOA}}(\mu_{\mathrm{s}},\mu_{\mathrm{v}},\phi)S-\rho_0(\mu_{\mathrm{s}},\mu_{\mathrm{v}},\phi)S} \tag{3}$$

Usually, Eq. (3) is used for atmospheric correction — calculating the surface reflectance from the apparent reflectance when the parameters (S, ρ_0, and T) are known.

Considering sun-satellite position conditions, the LUT was built by using 6S (Second Simulation of the Satellite Signal in the Solar Spectrum) or MODTRAN (MODerate resolution atmospheric TRANsmission) code to simulate different AODs with corresponding ρ_0, S and T. AODs can be retrieved by interpolating the LUT.

DDV method is based on two facts: first, the surface reflectances of dark pixel at red and blue bands are low and VIS/SWIR surface reflectance relationship is linear; second, at Short Wave Infrared (SWIR) band, aerosols are relatively transparent. But for the CCD aboard on CBERS02B does not include SWIR band, it is difficult to directly use DDV method in this paper to recognize dark pixel in the CCD images. Some modification about DDV algorithm is necessary before the AOD inversion based on CDD data.

For CCD sensor aboard on CBERS02B, the relationship between red and blue surface reflectances is established as Eq.(4),

$$\rho^{\mathrm{s}}_{\mathrm{red}}=k\rho^{\mathrm{s}}_{\mathrm{blue}} \tag{4}$$

where $\rho^{\mathrm{s}}_{\mathrm{red}}$ and $\rho^{\mathrm{s}}_{\mathrm{blue}}$ are respectively the surface reflectances of dark pixel at red and blue bands, k is VIS/SWIR ratio and it is set to 2 in the MODIS Algorithm Theoretical Basis Document (ATBD) of version 4.0. In this paper, the coefficient k is obtained through ground level measurements for different kinds of land covers. Then based on the reflectance relationship between red and blue bands, the LUT can be established using the radiative transfer code 6S. Finally, AOD is worked out by solving Eq.(5).

$$\begin{cases}\rho^{\mathrm{TOA}}_{\mathrm{blue}}(\mu_{\mathrm{s}},\mu_{\mathrm{v}},\phi)=\rho_0(\mu_{\mathrm{s}},\mu_{\mathrm{v}},\phi)+\dfrac{T(\mu_{\mathrm{s}})T(\mu_{\mathrm{v}})\rho^{\mathrm{s}}_{\mathrm{blue}}}{[1-\rho^{\mathrm{s}}_{\mathrm{blue}}S]}\\ \rho^{\mathrm{TOA}}_{\mathrm{red}}(\mu_{\mathrm{s}},\mu_{\mathrm{v}},\phi)=\rho_0(\mu_{\mathrm{s}},\mu_{\mathrm{v}},\phi)+\dfrac{T(\mu_{\mathrm{s}})T(\mu_{\mathrm{v}})\rho^{\mathrm{s}}_{\mathrm{red}}}{[1-\rho^{\mathrm{s}}_{\mathrm{red}}S]}\\ \rho^{\mathrm{s}}_{\mathrm{red}}=k\rho^{\mathrm{s}}_{\mathrm{blue}}\end{cases} \tag{5}$$

2.2 Dark pixel recognizing and ratio of blue/red

The key step in the modified DDV method in this paper is dark pixel recognizing and reflectance relationship establishing between blue and red bands for CBERS02B CCD sensor. Because of the lack of SWIR band, the NDVI (Kaufma & Sendra, 1988) is utilized to recognize dark pixel. As all known, the NDVI definition is as

$$\mathrm{NDVI}=\frac{\rho_{\mathrm{nir}}-\rho_{\mathrm{red}}}{\rho_{\mathrm{nir}}+\rho_{\mathrm{red}}} \tag{6}$$

where ρ_{nir} is the reflectance at near infrared band, and ρ_{red} is the reflectance at red band.

In September 2007, we measured the spectrums of six kinds of vegetation using Analytical Spectral Device (ASD), which include peanut, jasmine, cassava, mulberry, sugarcane and rice. The wavelength of spectral data ranges from 350nm to 2500nm with step of 1nm. In order to calculate the NDVIs of the different kinds of vegetation with the reflectances from the same bands as the CCD sensor, the band reflectances are computed by integrating the monochrome reflectances mentioned above with the channel respond functions of CCD according to Eq.(7)

$$R=\frac{\int_{\lambda 1}^{\lambda 2}S(\lambda)R(\lambda)\mathrm{d}\lambda}{\int_{\lambda 1}^{\lambda 2}S(\lambda)\mathrm{d}\lambda}=\frac{\sum_{i=0}^{N-1}S(\lambda_i)R(\lambda_i)\Delta\lambda}{\sum_{i=0}^{N-1}S(\lambda_i)\Delta\lambda} \tag{7}$$

where R is the band reflectance, $S(\lambda)$ and $R(\lambda)$ are spectral respond function and monochrome reflectance with wavelength λ. The spectral respond function for different bands is shown in Fig. 1. The results of band reflectance for CCD channels, the ratios of blue to red band reflectances and the relative NDVIs are list in the Table 1.

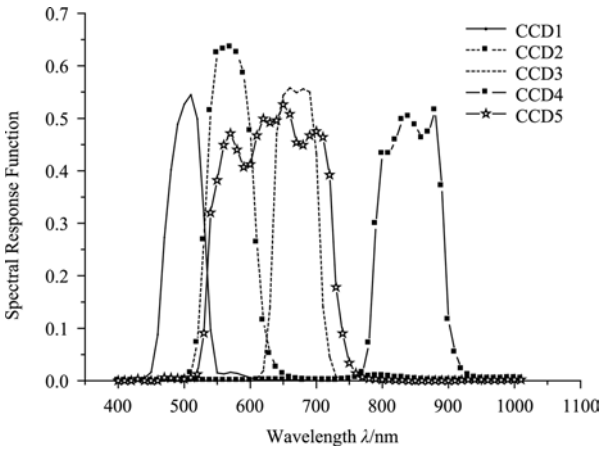

Fig. 1 Spectral response function of CCD sensor of CBERS02B

Table 1 The channel reflectances, ratio of blue to red band reflectances and the NDVI for different kinds of vegetations

Type	Number	Reflectance			Ratio of blue/red	NDVI
		CCD1	CCD3	CCD4		
Sugarcane	7	0.051	0.089	0.254	1.733	0.482
Peanut	1	0.035	0.052	0.326	1.491	0.726
Jasmine	7	0.025	0.040	0.377	1.582	0.809
Cassava	7	0.032	0.046	0.415	1.449	0.802
Mulberry	6	0.036	0.058	0.406	1.617	0.750
Rice	3	0.052	0.118	0.260	2.248	0.377

Table 1 illustrates that: (1) the NDVIs of peanut, jasmine, cassava and mulberry are very high, which range from 0.7 to 0.8 and the ratios of blue to red band reflectances for corresponding vegetations are near 1.4 to 1.6. (2) The NDVIs of sugarcane and rice are less than the others' but just the opposite

their ratios are more than those of other kinds of vegetations. The NDVI and ratio thresholds for dark pixel are respectively set to 0.7 and 1.55 based on the results shown in Table 1, it is assumed that the pixels with vegetation cover like peanut, jasmine, cassava and mulberry are recognized as dark pixels. But when the AOD inversion is implemented, the first step in the systematic project is to calculate the NDVI using the CCD measurements. As the NDVIs are directly calculated based on the apparent reflectances which including the atmosphere influence, the atmospheric effects caused by different AOD on NDVI for dark pixel recognizing are analyzed and the results are figured out in Fig. 2. Since the incident light path is a very important factor relative to atmospheric effects, four different solar zenith angles such as 10°, 20°, 40° and 60° as variable have been considered in our modified DDV method and the results are demonstrated in Fig. 2.

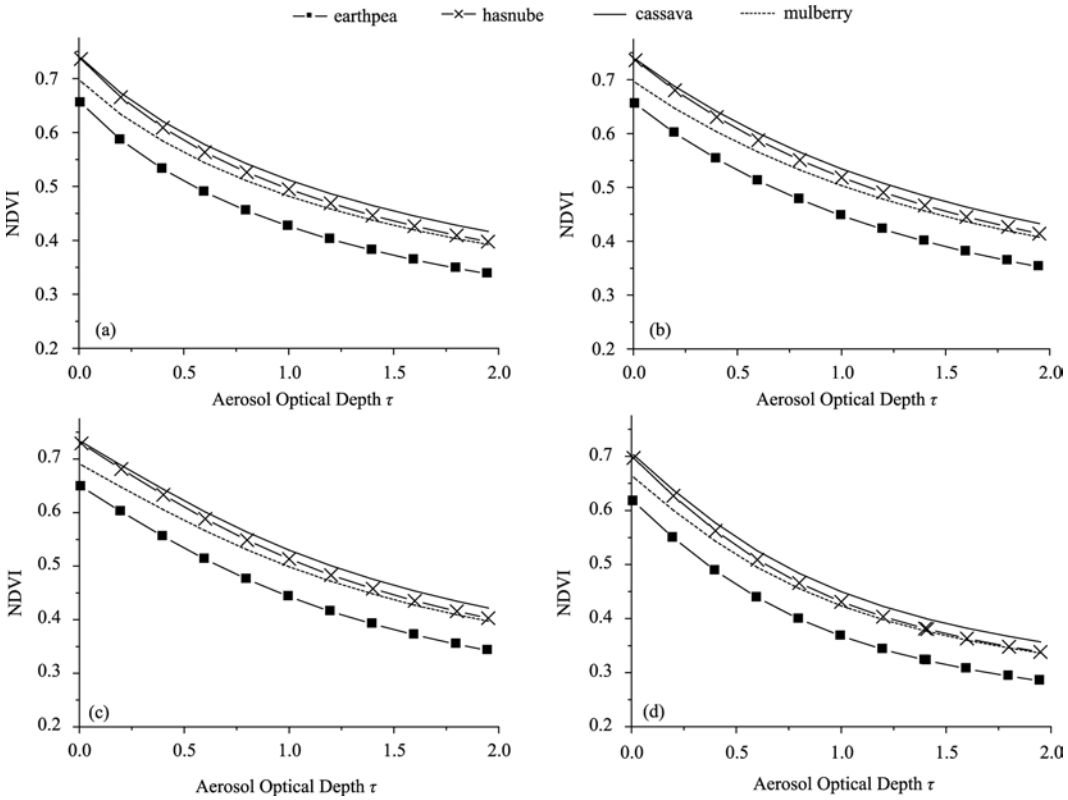

Fig. 2 The influence of atmosphere on NDVI
The sun zenith angles are 10° (a), 20° (b), 40° (c), and 60° (d)

As Fig. 2 shown, the AOD has great influences on NDVI including those of the dark pixel. The NDVIs resulting from the simulations for dark pixels with the vegetation cover such as earthpea, jasmine, cassava and mulberry decrease from 0.7 to 0.3 when the AOD increases from 0 to 2.0. So it is necessary to adjust the NDVI threshold from 0.7 to 0.3 in order to not miss the real dark pixel. Meanwhile the problem of fake dark pixel could be faced because of the low NDVI. The detail technique about fake dark pixel elimination will be illustrated in Section 3.3 of this paper.

3 AOD RETRIEVAL PROCEDURE

3.1 Building LUT

The LUT was built by 6S. 6S is a code with powerful functions, including the ability to simulate plane observations, deal with the case with elevated targets and non lambertian surface, etc (Vermote *et al*., 1997). The LUT contains pre-computed atmospheric optical properties (S, ρ_0, T) at three discrete wavelengths (red, blue and near infrared bands) for many different cases, which resulting from different inputing parameter, such as AOD, viewing geometry including solar zenith angle, sensor zenith angle and relative azimuth angle. The AOD is respectively set to 0.0, 0.1, 0.2, 0.4, 0.6 and 0.8, the solar zenith angles consist of 0.0°, 6.0°, 12.0°, 24.0°, 35.2°, 48.0°, 54.0°, 60.0° and 66.0°, the sensor zenith angles and relative azimuth angles were 0°. All of these properties are calculated assuming a surface reflectance of 0.

3.2 Data Pre-processing

Before the AOD retrieval, the data pre-processing includes two aspects. The first one is radiance calibration for CBERS02B CCD. Calibration coefficients obtained from field expriments in desert area in Inner Mongolia in October 2007 were used to calibrate the TOA reflectances calculated from CCD radiance data. The results showed the indeterminacy of the calibration was less than 6%. The second one is data resam-

pling from fine spatial resolution with 19.5m to coarse resolution with 195m in order to reduce signal to noise ratio (SNR) and speed the retrieving process.

3.3 AOD inversion process

The AOD was retrieved from CBERS02B CCD data as follow:

(1) Interpolate in LUT according to actual radiances and the solar elevation angle from the CBERS02B description files, then the corresponding optical properties S, ρ_0 and T at different AODs were worked out by linear interpolating method.

(2) Recognize the dark pixels by means of the NDVIs from the CCD measurements, and then the AOD of dark pixels with reflectance ratio of 1.55 were retrieved.

(3) Fake dark pixel elimination. Based on the atmospheric properties at band 3 and 4 obtained from the LUT, the atmospheric correction could be implemented by substituting the atmosphere properties into Eq.3, then the surface reflectances are worked out and further used to calculate the NDVIs. If the NDVI is less than 0.7, the pixel would be considered as fake dark pixel and it will be eliminated from the dark pixel.

4 RESULT VALIDATION AND ERROR ANALYSIS

4.1 Result validation

In order to validate the AODs retrieved using the modified DDV method developed in this paper, two CBERS02B CCD images respectively over Beijing on June 5th of 2008 and over Nanning on October 6th of 2007 were chosen in this test. Both AOD images were illustrated respectively in Fig. 3. Except some black pixels with no value because they are not dark pixel, the results show the AOD varies smoothly in both images.

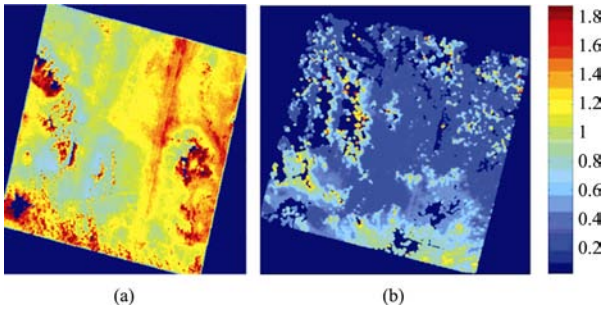

Fig. 3 The experimental images
(a) Retrieved AOD in Nanning area; (b) Retrieved AOD in Beijing area

Because of the lack of ground based AOD measurements while the satellite passing over, the validation of AOD inversed using the modified DDV method was carried out by comparing with MODIS AOD products. Because of the different spatial resolution and projection between MODIS AOD product and CBERS02B AOD product, for example, 10km spatial for MODIS AOD with no projection, but only 195m for CBERS02B AOD product with UTM projection, the AOD image from CBERS02B were resampled and re-projected to meet those of MODIS AOD product. The comparison of CBERS02B AOD with MODIS AOD is shown in Fig. 3. The results shows a good correlation between the two kinds of AODs, the correlation coefficient (R) was larger than 0.9 which are list in the last column in Table 2. Table 2 also illustrates the absolute and relative errors for both AOD products (Fig. 4).

Table 2 The retrieved aerosol optical depth from CBERS02B compared with MODIS aerosol products

Region	Number	Absolute error			Relative error/%			R
		Mean	Min	Max	Mean	Min	Max	
Nanning	59	0.310	0.226	0.385	29.5	20.9	40.6	0.715
Beijing	60	0.111	0.0007	0.646	26.4	0.07	149	0.772
Total	119	0.135	0.0007	0.646	21.1	0.07	149	0.910

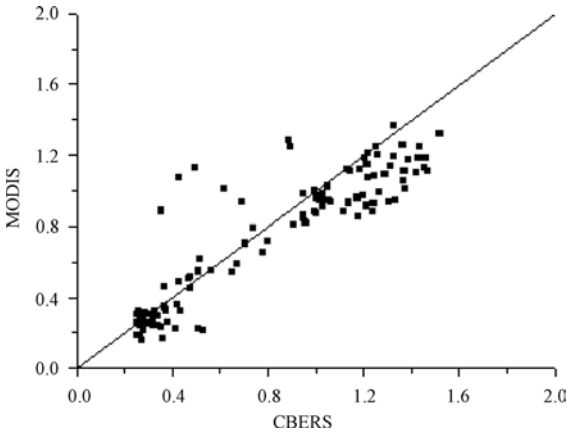

Fig. 4 Comparis on of the aerosol optical depth (AOD) between CBERS02B and MODIS

4.2 Errors brought by red to blue band reflectance ratio

The research revealed that the 0.01 error of surface reflectance may cause 0.1 error for AOD (Kaufman *et al*., 1997). It is necessary to study the errors brought by red to blue band reflectances ratio, which was set to a fixed value 1.55 for this modified DDV method. The maximum and minimum ratios listed in table are respectively 1.617 for mulberry and 1.449 for cassava, so three levels of ratio, which are 1.449, 1.55 and 1.617 respectively, had been used to simulate the influences caused by a fixed ratio based on 6S code. In this simulation, four different solar zenith angles 10°, 20°, 40° and 60° were used, and the simulated results were presented in Fig.5 and Table 3 respectively.

As shown in Fig.5 and Table 3, the errors resulting from the fixed ratio were small, and the mean error was only about 0.05. Although the maximal error was 0.19, the error kept stable even when the solar zenith angle and AOD increased.

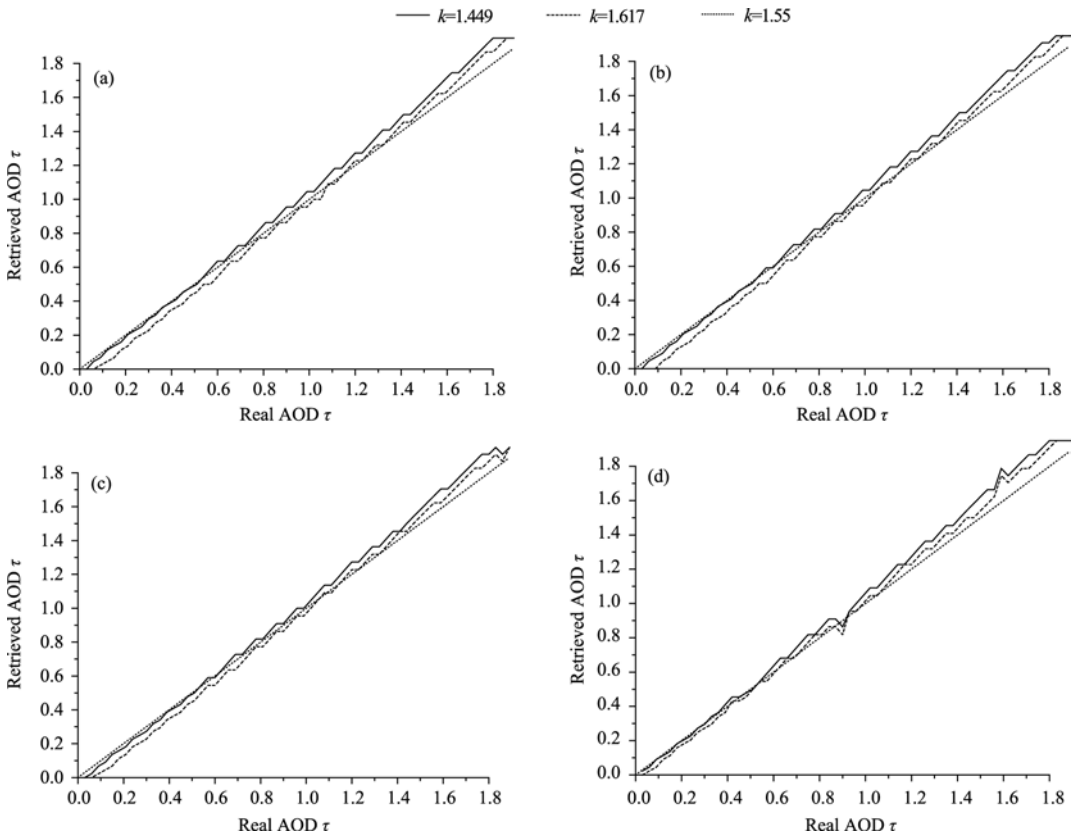

Fig. 5 The image of the influence of reflectance error on aerosol retrieval
The sun zenith angles are 10° (a), 20° (b), 40° (c), and 60° (d).

Table 3 The influence of reflectance error on aerosol retrieval

Sun Zenith /(°)	Ratio of blue/red	Absolute Error			*R*
		Mean	Max	Min	
10	*k*=1.449	0.0507	0.1500	0.0027	0.9996
	k=1.617	0.0442	0.0982	0.0018	0.9996
20	*k*=1.449	0.0478	0.1391	0.0027	0.9997
	k=1.617	0.0440	0.0900	0.0018	0.9997
40	*k*=1.449	0.0459	0.1391	0.0027	0.9996
	k=1.617	0.0409	0.0873	0.0018	0.9996
60	*k*=1.449	0.0621	0.1964	0.0010	0.9992
	k=1.617	0.0410	0.1555	0.0045	0.9992

5 CONCLUSION

The key important technique in DDV method is the dark pixel recognition based on the SWIR reflectance, but DDV can not be directly used for the CCD data because of the lack of the SWIR band. So the very important modification for DDV is how to develop the techniques combining NDVI, the ratio of red to blue band reflectances and their thresholds for dark pixels together in this paper. For the CCD data with fine spatial resolution aboard on CBERS02B satellite, a modified DDV method has been successfully used to retrieve the AOD. The conclusions are summarized as follows.

Firstly, the NDVI together with the ratio of red to blue band reflectances were used to judge the dark pixel. The shresholds are set to 0.7 and 1.55, respectively, for the dark pixel without the atmospheric effects.

Secondly, the NDVI calculated from apparent reflectance will be much lower than the NDVI threshold mentioned above because of the atmospheric effects for the actual CCD image. So based on the NDVIs resulted from the simulated reflectance under different AOD modules, the NDVI threshold for dark pixel discrimination in actual CCD image is modulated to 0.3.

After the AOD retrieval tests of CBERS02B over two different experiments areas, the AOD results were compared with MODIS AOD product and their errors analysis showed that the modified DDV method developed in this paper can be used to retrieve AOD from fine resolution CBERS02B data.

But a work left to do for the modified DDV method is the elevation effect on AOD, in which the molecular scattering effects should be corrected according to the actual elevation for each dark pixel. In addition, more tests are necessary to evaluate the modified DDV method availability for different seasons, especially in winter.

Acknowledgment: Thanks to the China Center for Resource Satellite Data and Applications (CRESDA) for CBERS02B Data and Atmosphere Archive and Distribution System (LAADS) for MODIS aerosol product. Many thanks to Ren Fujian, Liao Yongsheng, Zhu Junqi, Chen Jiang, Li Li and Wu Jiali for the field spectrum data.

REFERENCES

Duan M Z, Lu D R, Cui K J and Hao W Q. 2002. Retrieval of surface reflectance and aerosol optical thickness simultaneously from space measurement over land: basic theory and simulation. *Journal of Remote Sensing*, **6**(5): 321—327

Herman M, Deuze J L, Devaux C, Goloub P, Bréon F M and Tanré D. 1997. Romote sensing of aerosols over land surfaces including polarization measurements and application to POLDER measurements. *Journal of Geophysical Research*, **102**: 17039—17049

Hsu C N, Tsay S C, King M D and Herman J R. 2004. Aerosol properties over bright-reflecting. *IEEE Trans. Geosci. Remote Sens.*, **42**(3): 557—569

Kaufman Y J and Sendra C. 1988. Algorithm for automatic atmospheric corrections to visible and near-IR satellite imagery. *Int. J. Remote Sens.*, **9**: 1357—1381

Kaufman Y J, Tanré D, Remer L A, Vermote E F, Chu A and Holben B N. 1997. Operational remote sensing of tropospheric aerosol over land from EOS-Moderate Resolution Imaging Spectroradiometer. *J. Geophys. Res.*, **102**: 17051—17067

Li X J, Liu Y J, Qiu H and Zhang Y X. 2003. Retrieval method for optical thickness of aerosols over Beijing and its vicinity by using the MODIS data. *Acta Meteorologica Sinica*, **61**(5): 581—592

Mao J T, Li C C, Zhang J J, Liu X Y and Liu Q H. 2002. The comparison of remote sensing aerosol optical depth from MODIS data and ground sun-photometer observations. *Journal of Applied Meteorological Science*, **13**(U01): 127—135

Tanré D, Deschamps P Y, Devaux C and Herman M. 1988. Estimation of Saharan aerosol optical thickness from blurring effects in thematic mapper data. *J. Geophys. Res.*, **93**: 15955—15964

Vermote E F, Tanré D, Deuzé J L, Herman M and Morcrette J J. 1997. Second simulation of the satellite signal in the solar spectrum 6S: An overview. *IEEE Trans. Geosci. Remote Sens.*, **35**: 675—686

Wang L L, Xin J Y, Wang Y S, Li Z Q, Wang P C, Liu G R and Wen T X. 2007. Validation of MODIS aerosol products by CSHNET over China. *Chinese Science Bulletin*, **52**(12): 1708—1718

Wang X Q, Yang S Z, Zhu Y H and Yi W N. 2003. Aerosol optical thickness retrieval over land from MODIS data based on the inversion of the 6S Model. *Chniese Journal of Quantum Electronics*, **20**(5): 629—634

CBERS02B 卫星 CCD 传感器数据反演陆地气溶胶

王中挺[1,2], 陈良富[2], 巩 慧[2,3,4], 高海亮[2,3,4]

1. 环境保护部卫星环境应用中心, 北京 100029;
2. 遥感科学国家重点实验室, 中国科学院 遥感应用研究所, 北京 100101;
3. 国家航天局 航天遥感论证中心, 北京 100101;
4. 中国科学院 研究生院, 北京 100039

摘 要: 研究利用 CBERS02B 卫星的 CCD 传感器数据反演陆地气溶胶的方法。采用的方法是暗像元法。具体步骤为: 根据地面采集的植被光谱数据, 结合 CCD 传感器特点, 建立浓密植被(暗像元)红蓝波段(CCD 传感器的第三和第一波段)反射率与地表反射率之间的关系, 确定了暗像元识别的阈值, 讨论气溶胶光学厚度对暗像元识别的影响以及消除这种影响的方法; 利用 6S 进行辐射传输运算, 构建查找表; 根据 CBERS02B 卫星的 CCD 传感器数据, 从查找表插值得到气溶胶光学厚度, 并进行了算法的误差分析。用广西南宁市及北京地区附近的两景数据进行了实际的反演试验, 使用 MODIS 的气溶胶产品与反演结果进行比对。结果显示, CBERS02B 卫星的 CCD 传感器数据能够较好的反演陆地气溶胶。

关键词: 遥感, CBERS02B, 陆地气溶胶, 暗像元

中图分类号: P407/TP701 文献标识码: A

1 引 言

由于陆地气溶胶的物理化学性质多变, 时空分布高度不均一, 以及地表反射的影响, 利用卫星遥感气溶胶存在着较大的难度。目前, 监测陆地气溶胶的方法主要有暗目标法(Kaufman & Sendra, 1988)、结构函数法(Tanré 等, 1988)、基于地表反射率数据库(Hsu 等, 2004)的方法以及多角度偏振方法(Herman 等, 1997)等。目前, 利用遥感数据监测中国的气溶胶国内主要完成了以下的研究工作: MODIS 大气气溶胶产品在北京地区的验证(毛节泰等, 2002), 利用云下阴影实现陆地上空气溶胶和地表反射率的同时反演(段民征等, 2002), MODIS 数据的反演实验(王新强等, 2003), MODIS 数据对陆地气溶胶的反演方法的研究(李晓静等, 2003)。目前的气溶胶反演研究主要针对国外低空间分辨率卫星(以 MODIS 为主)开展, 而对国产的高空间分辨率卫星(如 CBERS)的研究开展得较少。

中巴地球资源卫星是 1988 年中国和巴西两国政府联合议定书批准, 在中国资源一号原方案基础上, 由中、巴两国共同投资, 联合研制的卫星(代号 China Brazil Earth Resources Satellite, 缩写 CBERS)。2007-09-19, 中巴资源卫星 02B (CBERS-02B)在太原卫星发射中心成功发射, 于 22 日上午 11 时成功接收到了 CBERS-02B 星首次开机成像的卫星影像数据。目前, 中巴地球资源卫星已广泛服务于中国国民经济的各个行业, 如农业、渔业、林业、环境等。自 2006-04-01 起, 中巴地球资源卫星数据实行免费网上分发。

作为高空间分辨率光学卫星, 精确的大气校正是 CBERS02B 卫星定量化应用的关键步骤, 而目前从其他卫星获得的气溶胶数据分辨率偏低(如 MODIS 为 10km), 不能很好的为 CBERS02B 卫星的大气校正服务, 如何利用 CBERS02B 卫星自身的数据反演获得气溶胶数据是迫切需要解决的问题。本文在 CBERS02B 卫星 CCD 传感器数据定标的基础上, 以广西省南宁地区及北京地区为试验区, 初步探讨 CBERS02B 卫星 CCD 传感器数据反演气溶胶

收稿日期: 2008-02-27; 修订日期: 2008-09-01

基金项目: 863 重大项目(编号: 2006AA06A303)和中国科学院知识创新工程重要方向项目(编号: kzcx1-yw-06-01)。

第一作者简介: 王中挺(1980—), 男, 河南郑州人, 博士, 工程师, 目前主要从事大气气溶胶遥感方面的研究工作。

光学厚度的可行性。

2 反演原理与算法

2.1 大气气溶胶反演原理

在地表朗伯体、大气水平均一假设条件下，卫星接收到的辐射 $L(\mu_v)$ 可以表达为(Vermote 等，1997):

$$L(\mu_v)=L_0(\mu_v)+\frac{r}{1-rS}\mu_s F_0 T(\mu_s)T(\mu_v) \tag{1}$$

式中，$\mu_s=\cos\theta_s$，$\mu_v=\cos\theta_v$。θ_s 与 θ_v 分别为太阳天顶角与观测天顶角；$L_0(\mu_v)$为观测方向的路径辐射项，r 为朗伯体地表反射率，S 为大气下界的半球反射率，T 为大气透过率，$\mu_s F_0$ 为大气层顶与太阳光垂直方向的辐射通量密度。

利用入射太阳辐射项 $F_0\mu_s$ 对式(1)进行归一化可得大气顶部反射率ρ_{TOA}:

$$\rho_{TOA}(\mu_s,\mu_v,\phi)=\rho_0(\mu_s,\mu_v,\phi)+\frac{T(\mu_s)T(\mu_v)\rho_s(\mu_s,\mu_v,\phi)}{[1-\rho_s(\mu_s,\mu_v,\phi)S]} \tag{2}$$

式中，ρ_0 是大气的路径辐射项等效反射率，ρ_s 为地表二向反射率，当地表为朗伯体时为 r。

将式(2)变化形式，转化为如下形式:

$$\rho_s(\mu_s,\mu_v,\phi)=\frac{\rho_{TOA}(\mu_s,\mu_v,\phi)-\rho_0(\mu_s,\mu_v,\phi)}{T(\mu_s)T(\mu_v)+\rho_{TOA}(\mu_s,\mu_v,\phi)S-\rho_0(\mu_s,\mu_v,\phi)S} \tag{3}$$

利用上式，可以利用大气参数 S，ρ_0，$T(\mu_s)T(\mu_v)$ 从表观反射率ρ_0 计算得到地表反射率ρ_s，也就是进行大气校正。

由于 $T(\mu_s)$，$T(\mu_v)$在式子中总是以乘积形式出现，因此将 $T(\mu_s)T(\mu_s)$作为一个参数考虑。实际反演中是用辐射传输模型，如 6S 或 MODTRAN 等计算假设的不同大气气溶胶模式和观测几何时，气溶胶光学厚度和 S，ρ_0，$T(\mu_s)T(\mu_v)$等 3 个参数之间的对应关系，据此建立查找表，通过查找表获取气溶胶光学厚度。暗像元法，也就是浓密植被法，原理为：(1)对于植被密集的具有较低反照率的地表(即暗像元)存在近红外通道反射率与红蓝通道反射率具有很好的线性相关；(2)气溶胶的影响在短波红外波段比在可见光波段小 15—30 倍，所以可被忽略不计。因此，可以从短波红外波段的表观反射率获得红蓝波段的地表反射率，然后从红蓝波段的表观反射率去除地表贡献，获得大气参数 S, ρ_0, $T(\mu_s)T(\mu_v)$，进而得到气溶胶光学厚度。

中巴资源卫星 02B 搭载有 CCD 相机、宽视场成像仪(WFI)和高分辨率相机(HR)。其中 CCD 相机包括 5 个波段：蓝、绿、红、近红外和全色波段，星下点地表分辨率为 19.5m。由于 CCD 相机没有短波红外波段，因此不能简单采用上面的方法进行暗像元识别和获得地表反射率，需按下面步骤进行反演。

对于CBERS02B星的CCD传感器，暗像元的红蓝波段的地表反射率存在固定的线性关系:

$$\rho^s_{red}=k\rho^s_{blue} \tag{4}$$

式中，ρ^s_{red}，ρ^s_{blue} 分别表示红光和蓝光波段浓密植被(暗像元)的地表反射率，对应 CCD 传感器的第 3 波段和第 1 波段，k 为红蓝地表反射率比率，在 MODIS 算法中一般设置为 2，对于 CBERS02B 卫星的 CCD 传感器则要根据传感器的特征，结合地面观测数据设定。在具体的反演过程中，大气参数 S，ρ_0，$T(\mu_s)T(\mu_v)$可以看作是大气气溶胶光学厚度的函数，将红、蓝波段的表观反射率 ρ^{TOA}_{red}，ρ^{TOA}_{blue} 代入式(2)得到 2 个方程，与式(3)结合，可以得到一个三元一次方程组，未知数为大气气溶胶光学厚度、红波段地表反射率 ρ^s_{red}、蓝波段地表反射率 ρ^s_{blue}。解这个方程组即可实现气溶胶光学厚度的反演。

$$\begin{cases}\rho^{TOA}_{blue}(\mu_s,\mu_v,\phi)=\rho_0(\mu_s,\mu_v,\phi)+\dfrac{T(\mu_s)T(\mu_v)\rho^s_{blue}}{[1-\rho^s_{blue}S]}\\ \rho^{TOA}_{red}(\mu_s,\mu_v,\phi)=\rho_0(\mu_s,\mu_v,\phi)+\dfrac{T(\mu_s)T(\mu_v)\rho^s_{red}}{[1-\rho^s_{red}S]}\\ \rho^s_{red}=k\rho^s_{blue}\end{cases} \tag{5}$$

2.2 暗像元特征提取

暗像元法的关键在于暗像元特征提取，即根据不同传感器的特点获得暗像元的识别方法，以及暗像元在红、蓝、短波近红外波段的地表反射率之间的关系。对于 CBERS02B 星的 CCD 传感器，由于没有相应的短波红外波段，采用归一化植被指数(NDVI)设定相应的阈值进行暗像元的选取(Kaufma & Sendra, 1988)，而红蓝波段地表反射率之间的关系需要从地面观测获得。

$$\mathrm{NDVI}=\frac{\rho_{nir}-\rho_{red}}{\rho_{nir}+\rho_{red}} \tag{6}$$

式中，ρ_{nir}，ρ_{red} 分别表示近红外和红光波段反射率，对应 CCD 传感器的第 3 波段和第 4 波段。

2007 年 11 月，我们利用 ASD 观测仪获取了大量的地面数据，其中包括花生、茉莉花、木薯、桑树、甘蔗、水稻等 6 种植被的光谱数据。ASD 观测

仪获得的数据波长为 350—2500nm，间隔 1nm；而 CBERS02B 的 CCD 传感器有 5 个波段，每个波段有不同的响应函数(图 1)。利用 CCD 传感器的不同波段的响应函数按照下式进行卷积，获得不同植被在各个波段的地表反射率，如表 1。

$$R=\frac{\int_{\lambda 1}^{\lambda 2}S(\lambda)R(\lambda)\mathrm{d}\lambda}{\int_{\lambda 1}^{\lambda 2}S(\lambda)\mathrm{d}\lambda}=\frac{\sum_{i=0}^{N-1}S(\lambda_i)R(\lambda_i)\Delta\lambda}{\sum_{i=0}^{N-1}S(\lambda_i)\Delta\lambda} \quad (7)$$

式中，$S(\lambda_i)$ 表示传感器各波段的响应函数、$R(\lambda_i)$ 为对应波段的反射率。

从表 1 可以看出，花生、茉莉花、木薯、桑树的 NDVI 较为接近，在 0.7—0.8 附近，同时红蓝波段比率也比较接近，在 1.4—1.6 之间；甘蔗、水稻的 NDVI 值要远远小于其他 4 种，红蓝波段比率变动也比较大，并不适合作为暗像元。因此，暗像元的 NDVI 阈值可以设置 0.7，红蓝波段比率设置为 1.55。

表 **1** 植被光谱数据

地表类型	观测数目	地表反射率			红蓝波段比率	NDVI
		CCD1	CCD3	CCD4		
甘蔗	7	0.051	0.089	0.254	1.733	0.482
花生	1	0.035	0.052	0.326	1.491	0.726
茉莉花	7	0.025	0.040	0.377	1.582	0.809
木薯	7	0.032	0.046	0.415	1.449	0.802
桑树	6	0.036	0.058	0.406	1.617	0.750
水稻	3	0.052	0.118	0.260	2.248	0.377

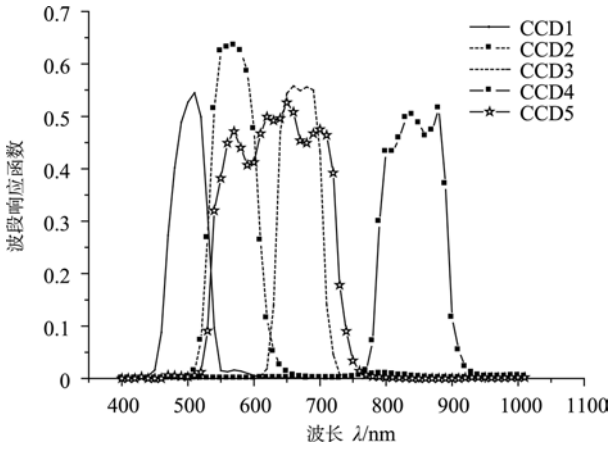

图 1 CBERS02B 星 CCD 传感器的波段响应函数

但在可见光(包括红光)与近红外波段，卫星接收到的反射率并非地表反射率，而是受到大气影响的表观反射率，利用表观反射率获得的 NDVI 会受到大气的影响。图 2 为利用 6S 模拟大气状况，计算得到 S, ρ_0,$T(\mu_s)T(\mu_v)$3 个大气参数，利用式(2)计算得到红波段和近红外波段的表观反射率，然后计算 NDVI 值。

从图 2 中可以看出，大气尤其是气溶胶对植被的 NDVI 会有很大的影响，在气溶胶光学厚度达到 2

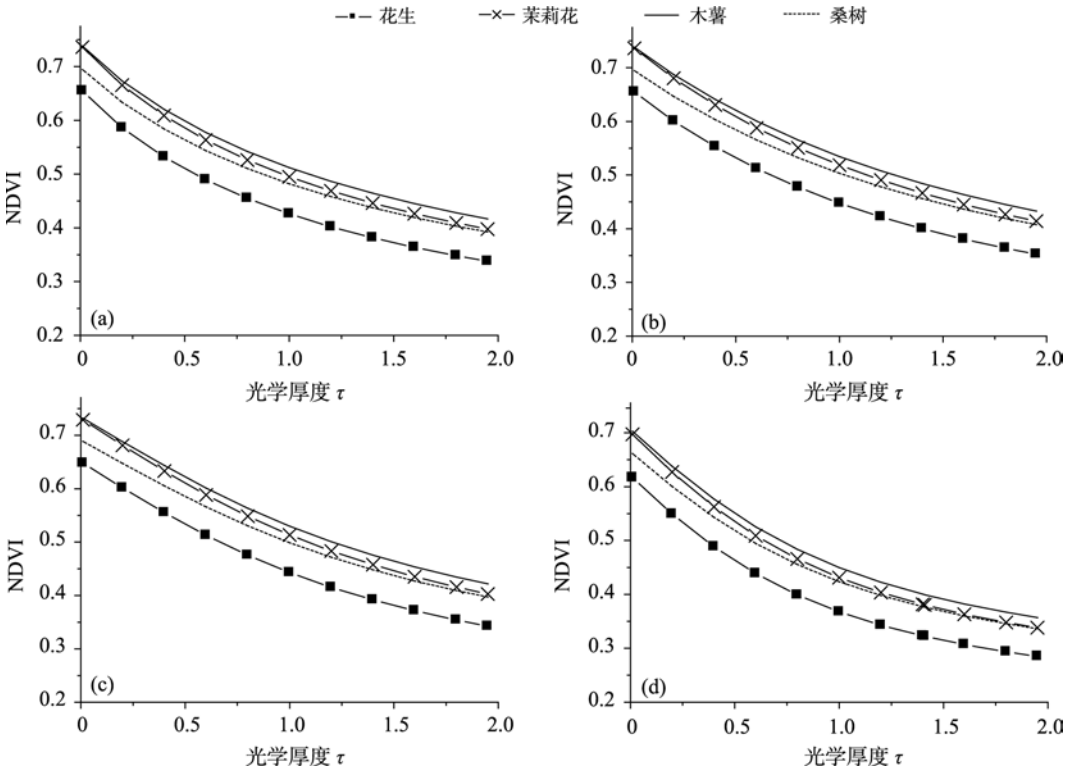

图 2 不同大气条件对植被 NDVI 的影响

(a)太阳天顶角为 10°; (b)太阳天顶角为 20°; (c) 太阳天顶角为 40°; (d) 太阳天顶角为 60°，观测天顶角和相对方位角统一设置为 0°

时，会使 NDVI 从 0.7 降低到 0.3 左右。考虑到大气对 NDVI 的影响，暗像元的阈值设置为 0.3。将阈值设低，可能会使某些不是暗像元的点也被判别为暗像元，还需在反演结束时，根据得到的气溶胶光学厚度值做进一步的处理，以剔除非暗像元数据。

3 数据处理流程

3.1 查找表构建

查找表的构建使用 6S 软件设定相应的参数进行辐射传输计算得出。6S(the Second Simulation of the Satellite Signal in the Solar Spectrum)是在 5S 的基础上，由 Vermote 等改进。它是利用连续阶散射(Successive Orders of Scattering)方法对大气辐射传输过程进行计算的软件，能够处理吸收气体(水汽、臭氧、甲烷、二氧化氮等)，并能对非朗伯地表进行处理(Vermote 等, 1997)。

利用 6S 进行辐射传输计算时，要设定不同的几何参数、气溶胶参数、波段、地表参数。几何参数: 太阳天顶角 9 个(0°, 6°, 12°, 24°, 35.2°, 48°, 54°, 60°, 66°)，观测天顶角和相对方位角设为 0°(CBERS02B 的 CCD 传感器观测天顶角与视场角较小，可以看作垂直观测)；气溶胶参数: 大陆型气溶胶，0.55μm 的光学厚度 6 个(0, 0.25, 0.5, 1, 1.5, 1.95)；波段: CCD 传感器的第 1、第 3 波段和第 4 波段，即蓝光、红光和近红外波段；地表参数: 海拔为 0m，地表类型为植被。

3.2 数据预处理

在进行气溶胶反演时，需要对获得的图像进行预处理，包括 2 个方面的工作: (1)重采样。CBERS02B 星的 CCD 传感器的星下点分辨率为 19.5m，对于反演大气气溶胶分辨率过细，不仅使反演容易受到地表地形起伏影响，同时会带来较大的噪声，而且会大大延缓反演速度。因此，在运算之前，对图像进行 10×10 的合成，重采样为 195m 分辨率的图像。(2)辐射定标。2007 年 10 月，中国科学院遥感应用研究所论证中心在达里湖贡戈尔草原进行场地在轨定标试验，对 CBERS02B 卫星搭载的传感器进行辐射定标，并获得相应的定标系数，其中 CCD 传感器的定标精度小于 6%。本文的定标系数采用的就是这次试验的结果。

3.3 气溶胶光学厚度的反演

在获得查找表和图像的表观反射率数据后，按照下面的步骤进行气溶胶反演计算:

(1)查找表插值。从图像的描述文件中读取的太阳高度角 $\theta_{\text{sun\_elevation}}$，进而计算得到太阳天顶角 $\theta_{\text{sun\_zenith}}$，在查找表选取相应的数据，按照太阳天顶角进行线性插值，得到第 1 波段、第 3 波段和第 4 波段的不同气溶胶光学厚度的ρ_0，$T(\mu_s)T(\mu_v)$和 S 参数。

(2) 计算暗像元气溶胶。按照式(4)，从图像第 3 波段和第 4 波段的表观反射率计算图像的 NDVI，根据阈值选取暗像元。按照不同的光学厚度插值ρ_0，$T(\mu_s)T(\mu_v)$和 S 参数，代入式(3)中计算第 1 波段和第 3 波段的地表反射率；然后计算所得的第 1、第 3 波段的地表反射率是否满足式(4)要求，相差最小的气溶胶光学厚度值即为所求。

(3) 剔除非暗像元点。考虑到大气的影响，选取暗像元的 NDVI 阈值是在大气影响最大的情况下确定的。而实际情况中，由于大气条件很少满足极端的情况(也就是气溶胶光学厚度达到 2)，会有部分非暗像元被误判为暗像元。因此，需要根据反演的结果进行检验，以剔除非暗像元点。首先，利用反演得到的气溶胶光学厚度值和太阳天顶角对查找表进行插值，得到第 3 波段和第 4 波段的大气参数；然后，将大气参数和表观反射率代入式(3)进行大气校正，得到地表反射率；最后，根据地表反射率计算 NDVI，将大气校正后 NDVI 小于 0.7 的非暗像元点剔除。

4 结果比对与误差分析

4.1 结果比对

按照上述的方法对 2007 年 10 月 6 日广西南宁附近和 2008 年 6 月 5 日北京附近的两景数据进行了反演试验，结果如图 3 所示。

从图 3 可以看到，气溶胶光学厚度南宁地区的

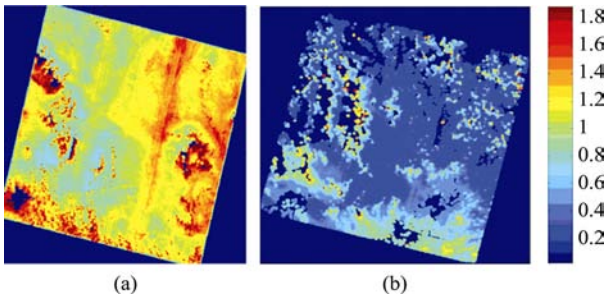

图 3 反演试验图

(a)南宁地区结果; (b)北京地区结果

值偏大，而北京地区的值偏小；同时分布比较均匀，变化缓慢，符合气溶胶局域变化特征。因此，可以认为本算法能够反映气溶胶的变化特征。反演结果图像中出现许多的空白之处，是因为将不符合暗像元要求的地物(如云、裸土、水体等)的气溶胶光学厚度设置为零的原因。

由于没有过境时获得相应的地基气溶胶观测数据，采用 MODIS 的气溶胶产品与本文反演结果进行比对，以得出反演结果的精度进行部分的评价。MODIS 气溶胶算法比较成熟，国内外已有多人进行过验证工作，研究表明，在中国境内的农业生态区域 MODIS 能够获得较高的精度(Wang 等, 2007)。

MODIS 气溶胶产品的分辨率为 10km，本文计算出 CBERS02B 的 CCD 传感器获得的分辨率为 195m，而且二者的投影方式不同。因此，对获得的结果完成重采样和配准工作，将分辨率采样为 10km，然后与 MODIS 产品进行比较，得到结果如图 4、表 2。

表 2　反演结果与 **MODIS** 气溶胶产品比较表

地区	有效观测数	绝对误差			相对误差/%			相关系数
		平均值	最小值	最大值	平均值	最小值	最大值	
南宁	59	0.310	0.226	0.385	29.5	20.9	40.6	0.715
北京	60	0.111	0.0007	0.646	26.4	0.07	149	0.772
合计	119	0.135	0.0007	0.646	21.1	0.07	149	0.910

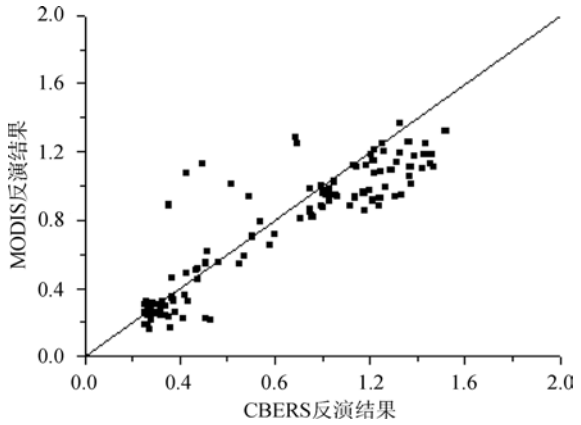

图 4　CBERS02 反演气溶胶光学厚度结果与 MODIS 产品比较图

从比较结果来看，本算法获得的结果与 MODIS 有较高的相关系数，结果基本可以满足精度要求。但绝对误差比较大，可能是以下原因造成的：(1)二者分辨率不同，重采样带来误差；(2)气溶胶模式不同，本文采用的是大陆型气溶胶，而 MODIS 则是粗细粒子组合的形式。

4.2　误差分析

在确定红蓝波段地表反射率关系时，红蓝波段地表反射率比率 k 设为一个固定值。虽然暗像元的地表反射率较低，但研究表明，地表反射率 0.01 的误差会带来气溶胶光学厚度 0.1 的误差(Kaufman 等, 1997)。因此，需要对红蓝波段地表反射率比率带来的误差做进一步的讨论。

根据 2.2 节中的计算结果，植被红蓝波段地表反射率比率最大值为 1.617，最小值为 1.449，分别对应桑树和木薯 2 种类型的植被。利用这 2 种植被的地表反射率数据，模拟不同的大气状况，利用 6S 进行辐射传输运算，产生相应的模拟数据，然后使用本算法进行反演，得到的结果如图 5 和表 3。观测天顶角和相对方位角设置为 0°。

从图 5 和表 3 可以看出，暗像元地表反射率带来的误差较小，虽然有最大为 0.19 的误差，但平均值在 0.05 附近，总体可以将误差控制在 0.1 的范围之内；而且随着太阳天顶角以及气溶胶光学厚度的增大，误差并没有发生明显的变化。

表 3　红蓝波段地表反射率比率误差对反演结果影响表

太阳天顶角/(°)	红蓝波段地表反射率比率	绝对误差			相关系数
		平均值	最大值	最小值	
10	k=1.449	0.0507	0.1500	0.0027	0.9996
	k=1.617	0.0442	0.0982	0.0018	0.9996
20	k=1.449	0.0478	0.1391	0.0027	0.9997
	k=1.617	0.0440	0.0900	0.0018	0.9997
40	k=1.449	0.0459	0.1391	0.0027	0.9996
	k=1.617	0.0409	0.0873	0.0018	0.9996
60	k=1.449	0.0621	0.1964	0.0010	0.9992
	k=1.617	0.0410	0.1555	0.0045	0.9992

5　结论与讨论

利用暗像元法对 CBERS02B 卫星的 CCD 传感器数据进行了陆地气溶胶的反演研究。主要完成了以下的工作，并获得了相应的结论：

(1) CCD 传感器数据具有红光和蓝光波段，浓密植被在这两个波段较低的地表反射率及其之间的线性关系为气溶胶光学厚度的反演提供了可能；但 CCD 传感器数据缺失相应的短波红外数据，也为暗像元的提取与暗像元地表反射率确定造成了困难；

(2) 利用地面观测数据，针对 CBERS02B 星的 CCD 传感器，提取了暗像元的特征，即暗像元识别的阈值与红蓝波段地表反射率比率；

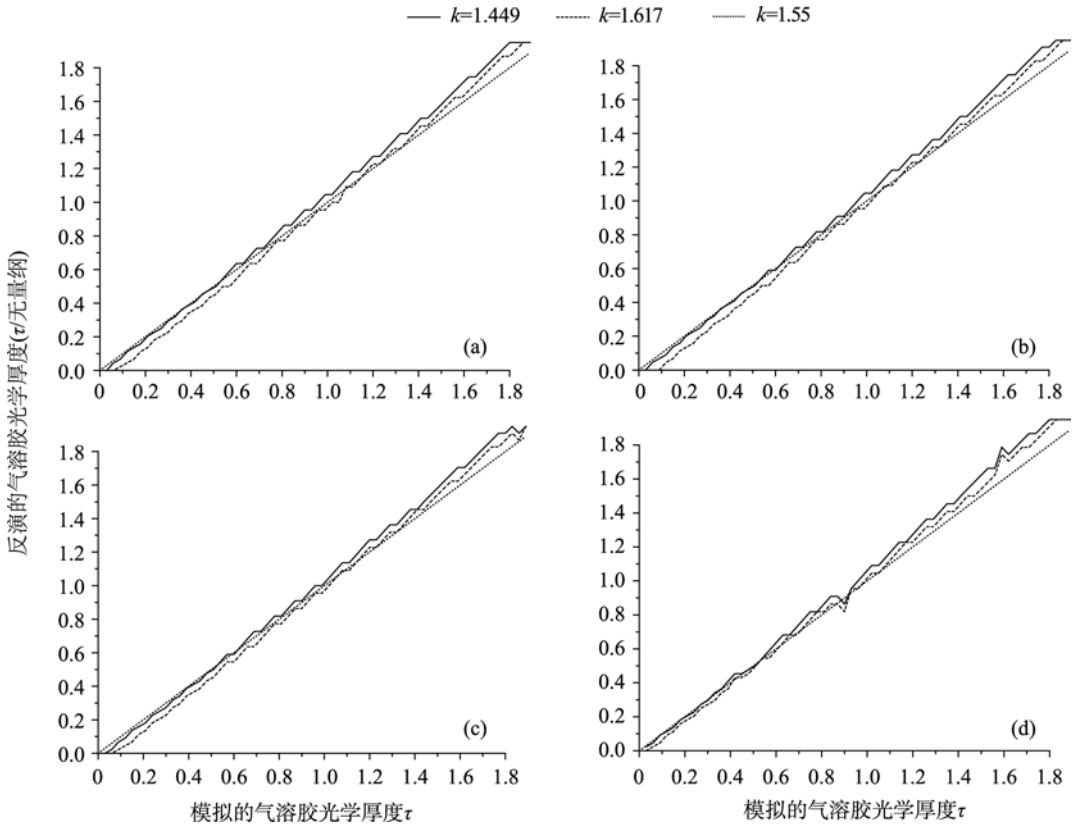

图 5　红蓝波段地表反射率比率误差对气溶胶反演的影响

(a)太阳天顶角为 10°; (b) 太阳天顶角为 20°; (c) 太阳天顶角为 40°; (d) 太阳天顶角为 60°

(3) 讨论了大气对暗像元识别的影响，提出了剔除非暗像元的方法，即先假定反演结果是正确的，利用反演的气溶胶光学厚度值进行大气校正，获得不受大气影响的 NDVI 值，剔除小于 0.7 的像元;

(4) 对算法进行了误差分析，结果表明暗像元地表反射率关系的误差对反演结果的影响较小，在可以接受范围之内;

(5) 利用 MODIS 气溶胶产品与算法反演结果进行了比对，得出在南方和北方不同地区本算法的精度都能够满足需求。

当然，本研究也存在着不足之处。查找表的海拔高度设置为 0，没有考虑到随着海拔的变化、大气分子光学厚度的变化带来的影响；暗像元的地表反射率关系的确定采用的地基观测数据比较有限，还需要更多季节和更多地区的观测数据以进行进一步的探讨；暗像元法适用于植被比较茂密的地区，在中国北方冬季时或者西北荒漠地区，算法会失效，需考虑其他办法反演气溶胶。

致　谢　本文使用的CBERS02B卫星数据由中国资源卫星应用中心提供，MODIS 气溶胶产品由 LAADS(the Level 1 and Atmosphere Archive and Distribution System)提供，地面 ASD 观测数据由广西省测绘局任建福、廖永生、朱俊琦同志和河南理工大学的陈江同学以及中国科学院遥感应用研究所的李丽、武佳丽同学协助获得，在此表示感谢。

REFERENCES

Duan M Z, Lu D R, Cui K J and Hao W Q. 2002. Retrieval of surface reflectance and aerosol optical thickness simultaneously from space measurement over land: basic theory and simulation. *Journal of Remote Sensing*, **6**(5): 321—327

Herman M, Deuze J L, Devaux C, Goloub P, Bréon F M and Tanré D. 1997. Romote sensing of aerosols over land surfaces including polarization measurements and application to POLDER measurements. *Journal of Geophysical Research*, **102**: 17039—17049

Hsu C N, Tsay S C, King M D and Herman J R. 2004. Aerosol properties over bright-reflecting. *IEEE Trans. Geosci. Remote Sens.*, **42**(3): 557—569

Kaufman Y J and Sendra C. 1988. Algorithm for automatic atmospheric corrections to visible and near-IR satellite imagery. *Int. J. Remote Sens.*, **9**: 1357—1381

Kaufman Y J, Tanré D, Remer L A, Vermote E F, Chu A and Holben B N. 1997. Operational remote sensing of tropospheric aerosol over land from EOS-Moderate Resolution Imaging Spectroradiometer. *J. Geophys. Res.*, **102**: 17051—17067

Li X J, Liu Y J, Qiu H and Zhang Y X. 2003. Retrieval method for optical thickness of aerosols over Beijing and its vicinity by using the MODIS data. *Acta Meteorologica Sinica*, **61**(5): 581—592

Mao J T, Li C C, Zhang J J, Liu X Y and Liu Q H. 2002. The comparison of remote sensing aerosol optical depth from MODIS data and ground sun-photometer observations. *Journal of Applied Meteorological Science*, **13**(U01): 127—135

Tanré D, Deschamps P Y, Devaux C and Herman M. 1988. Estimation of Saharan aerosol optical thickness from blurring effects in thematic mapper data. *J. Geophys. Res.*, **93**: 15955—15964

Vermote E F, Tanré D, Deuzé J L, Herman M and Morcrette J J. 1997. Second simulation of the satellite signal in the solar spectrum 6S: An overview. *IEEE Trans. Geosci. Remote Sens.*, **35**: 675—686

Wang L L, Xin J Y, Wang Y S, Li Z Q, Wang P C, Liu G R and Wen T X. 2007. Validation of MODIS aerosol products by CSHNET over China. *Chinese Science Bulletin*, **52**(12): 1708—1718

Wang X Q, Yang S Z, Zhu Y H and Yi W N. 2003. Aerosol optical thickness retrieval over land from MODIS data based on the inversion of the 6S Model. *Chniese Journal of Quantum Electronics*, **20**(5): 629—634

附中文参考文献

段民征, 吕达仁, 崔克俭, 郝文强. 2002. 利用云下阴影实现陆地上空气溶胶和地表反射率的同时反演——理论方法和模拟. 遥感学报, **6**(5): 321—327

李晓静, 刘玉洁, 邱红, 张玉香. 2003. 利用 MODIS 资料反演北京及其周边地区气溶胶光学厚度的方法研究. 气象学报, **61**(5): 581—592

毛节泰, 李成才, 张军华, 刘晓阳, 刘启汉. 2002. MODIS 卫星遥感北京地区气溶胶光学厚度及与地面光度计遥感的对比. 应用气象学报, **13**(U01): 127—135

王新强, 杨世植, 朱永毫, 易维宁. 2003. 基于 6S 模型从 MODIS 图像反演陆地上空大气气溶胶光学厚度. 量子电子学报, **20**(5): 629—634